Biochimica et Biophysica Acta xxx (2015) xxx–xxx

Contents lists available at ScienceDirect

Biochimica et Biophysica Acta

journal homepage: www.elsevier.com/locate/bbagen

Formation of fluorophores from the kynurenine pathway metabolite *N*-formylkynurenine and cyclic amines involves transamidation and carbon–carbon bond formation at the 2-position of the amine

Petr Tomek, Brian D. Palmer, Jackie D. Kendall, Jack U. Flanagan, Lai-Ming Ching *

Auckland Cancer Society Research Centre, Faculty of Medical and Health Sciences, School of Medicine, University of Auckland, Auckland, New Zealand

ARTICLE INFO

Article history:
Received 26 February 2015
Accepted 13 April 2015
Available online xxxx

Keywords:
Indoleamine 2,3-dioxygenase
N-formylkynurenine
Tryptophan catabolism
Transamidation
Piperidine
Fluorophore

ABSTRACT

Background: Tryptophan catabolism along the kynurenine pathway is associated with a number of pathologies including cataract formation and cancer. Whilst the chemical reactions of kynurenine are well studied, less is known about the reactivity of its precursor *N*-formylkynurenine (NFK). We previously reported the generation of a strong fluorophore in an aqueous reaction of NFK with piperidine, and herein we describe its structure and mechanism of formation.
Methods: Compounds were identified using NMR, mass and UV spectroscopic techniques. The products from the reaction of amines with amino acids were quantified using HPLC-MS.
Results: The novel fluorophore was identified as a tetrahydroquinolone adduct (PIP-THQ), where piperidine is *N*-formylated and attached at its 2-position to the quinolone. NFK is initially deaminated to generate an unsaturated enone, which forms an adduct with piperidine and is subsequently converted into the fluorophore. Testing of a variety of other secondary amines showed that only cyclic amines unsubstituted at both positions adjacent to nitrogen could form fluorophores efficiently. The amino acids tryptophan and kynurenine, which lack the formamide group do not form such fluorophores.
Conclusions: NFK forms fluorophores in a not previously published reaction with cyclic amines.
General significance: Our study is the first to provide evidence for concurrent transamidation and substitution at the 2-position of a cyclic amine occurring under moderately-heated aqueous conditions with no added catalysts. The high reactivity of NFK demonstrated here could result in formation of biologically relevant metabolites yet to be characterised.

1. Introduction

The kynurenine pathway is a major tryptophan (TRP) catabolic route in humans [1,2]. In this pathway, TRP is firstly oxidised into *N*-formylkynurenine (NFK) by haem enzymes indoleamine 2,3-dioxygenase 1 (IDO1) and tryptophan 2,3-dioxygenases (TDO), [3] and then hydrolysed into kynurenine (KYN) by kynurenine formamidase [4]. Further enzymatic conversion of KYN ultimately leads to production of the cofactor nicotinamide adenine dinucleotide [1]. KYN can also spontaneously deaminate at physiological pH to form a reactive α,β-carboxyketoalkene (KYN-CKA) [5] which can either form adducts with biological nucleophiles [6,7], undergo reduction or cyclise to form kynurenic acid or kynurenine yellow (Scheme 1) [8–10].

The kynurenine pathway has recently attracted intense interest due to its central role in causing tumour mediated immune suppression [11]. IDO1 has been found in a broad range of human tumours causing local depletion of TRP and accumulation of KYN, which result in accumulation of T regulatory suppressor cells and inactivation of T effector cells [12,13]. High IDO1 expression in tumours is associated with poor prognosis for cancer patients [14–17]. Blocking IDO1 activity using small-molecule inhibitors is now a recognised approach for cancer therapy [18–20] and two IDO1 inhibitors are currently showing promise in human clinical trials [21,22].

Abbreviations: 2-MePIP, (2-methylpiperidine); 3-MePIP, (3-methylpiperidine); 4-MePIP, (4-methylpiperidine); AZP, (azepane); DEA, (diethylamine); DMP, (cis-2,6-dimethylpiperidine); DPA, (dipropylamine); HRMS, (high-resolution mass spectrometry); IDO1, (indoleamine 2,3-dioxygenase 1); KYN, (kynurenine); KYN-CKA, (kynurenine α,β-carboxyketoalkene); NFK-CKA, (*N*-formylkynurenine α,β-carboxyketoalkene); MQW, (Milli-Q water); MW, (molecular weight); NFK, (*N*-formylkynurenine); NMePIP, (*N*-methylpiperidine); NMePYR, (*N*-methylpyrrolidine); PIP, (piperidine); PYR, (pyrrolidine); R_t, (retention time); TDO, (tryptophan 2,3-dioxygenase); TFA, (trifluoroacetic acid); THQ, (tetrahydroquinolone); TMP, (2,2,6,6-tetramethylpiperidine); TRP, (tryptophan).

* Corresponding author at: Auckland Cancer Society Research Centre, Faculty of Medical and Health Sciences, University of Auckland, Auckland, New Zealand. Tel.: +64 9 373 7599x86140.
E-mail address: l.ching@auckland.ac.nz (L.-M. Ching).

http://dx.doi.org/10.1016/j.bbagen.2015.04.007
0304-4165/

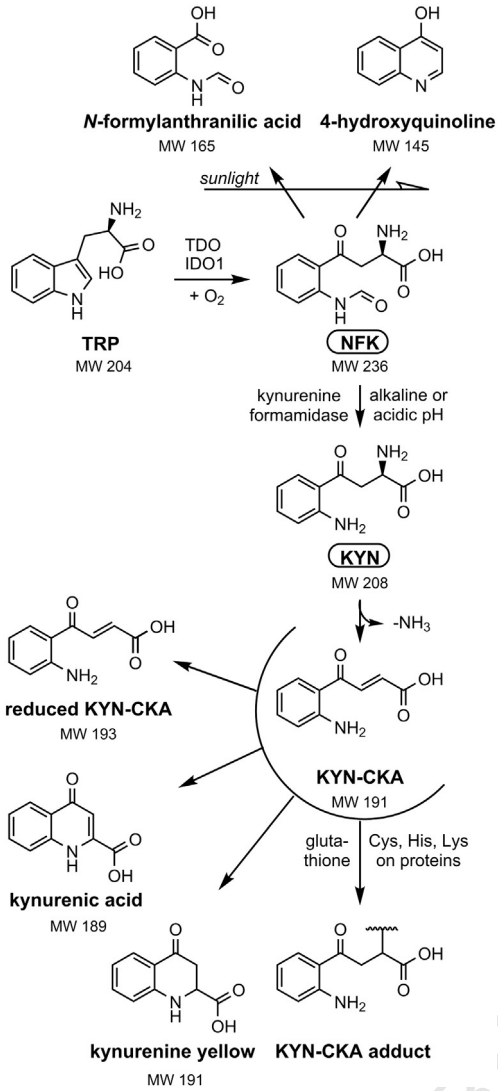

Scheme 1. Overview of major chemical transformations of KYN and NFK. MW stands for molecular weight in Daltons.

Testing of compounds for IDO1 inhibitory activity in the past has relied on a colorimetric assay introduced in 1988 [23]. In this assay, the NFK produced from IDO1-catalysed conversion of TRP is firstly hydrolysed to KYN in trichloroacetic acid and then reacted with *p*-dimethylaminobenzaldehyde to form a Schiff base and quantified at 480 nm. The IDO1 fluorescence assay introduced in 2006 measures fluorescence of KYN produced from hydrolysis of NFK in sodium hydroxide [24]. The sensitivity of this fluorescence assay is comparable to that of the original absorbance assay, but has the advantage of requiring only a single step incubation at 65 °C with sodium hydroxide. We recently developed a fluorescence assay with 30-fold better sensitivity than the previous assays for measuring IDO1 activity. In this new assay, NFK is converted into a strong fluorophore in a reaction at 65 °C with cyclic amine piperidine (PIP) [25]. To our knowledge, the formation of fluorophore from NFK has not been reported, and the only published transformation of NFK is photooxidation into *N*-formylanthranilic acid and 4-hydroxyquinoline [26]. In this communication we report on the isolation and characterisation of the chemical structure of the novel fluorophore which we have called piperidine-tetrahydroquinolone (PIP-THQ) and provide experimental evidence for a previously unreported chemical transformation pathway leading to its formation.

2. Materials and methods

2.1. Materials

DL-Kynurenine (>95%, cat. no. 69791) obtained from AK Scientific (Union City, CA, USA) with only 62% purity by HPLC compared to crystalline L-Kynurenine (cat. no. K8625) from Sigma-Aldrich (St Louis, MO, USA), was used with no further purification. ^{13}C-labelled formic acid (99%, cat. no. 14C-428) was purchased from Cambridge Isotope Laboratories. All other chemicals were obtained from Merck or Sigma-Aldrich.

2.2. General analytical methods

NMR spectra were obtained on a Bruker Avance 400 spectrometer at 400 MHz for ^{1}H and 100 MHz for ^{13}C spectra and were referenced to tetramethylsilane. High resolution mass spectra were determined on a Bruker micrOTOF-Q mass spectrometer (HRMS) operating under electrospray ionisation conditions. LC-MS analyses were carried out on Agilent 1100 HPLC/6150 single quadrupole electrospray mass spectrometer. Ionisation conditions were: drying gas temperature 270 °C, gas flow 10 L/min, nebulizer pressure gauge 35 psi, capillary voltage +3 kV and −3 kV, and fragmentor voltage 70 V. Spectra were acquired over 107–1000 *m/z* range. Analytical separations were carried out on a Luna C_{18} column (5 μm, 100 A, 150 × 2 mm; Phenomenex, Torrance, CA, USA) eluted using 80% acetonitrile (MeCN) (A) and Milli-Q water (MQW) containing 25 mM formic acid (pH ~2.7) (B) in a binary gradient: 0 min (5% A), 11 min (58% A), 14–17 min (96% A), 18–22 min (5% A) at flow rate 0.4 mL/min and 40 °C. UV/VIS chromatograms were acquired using diode-array detection at multiple wavelengths simultaneously ranging from 240 to 400 nm, and fluorescence signals were acquired at emission and excitation wavelengths of 500 nm and 400 nm, respectively, using an in-line fluorescence detector. Data were analysed on Agilent Chemstation software.

The purity of isolated compounds was determined by HPLC analysis (from 254 nm chromatogram) as a peak area of compound of interest divided by the peak area of all analysed peaks in the chromatogram. Peak selection was performed manually in Agilent Chemstation software.

Mass fragmentation experiments were performed on an Agilent 1200 HPLC/6460 triple quadrupole mass spectrometer equipped with Agilent JetStream electrospray ionisation interface (drying gas temperature 250 °C, flow 10 L/min, nebulizer pressure 40 psi, capillary voltage +2.75 kV and −3.5 kV, sheath gas temperature 250 °C, sheath gas flow 6 L/min, collision cell accelerator voltage 7 V, fragmentor voltage was 50 V and 135 V for MS2 scans and MS/MS fragmentation experiments, respectively). MS2 scans were acquired over the 50–1000 *m/z* range. Samples were injected into LC-MS with no column in a mobile phase consisting of solution A (4.5 mM ammonium formate pH 3.5) and solution B (0.1% (*v/v*) formic acid in MeCN in ratio 6:4 (A:B) and at a flow rate 0.3 mL/min). Data were analysed in Agilent MassHunter software.

Fluorescence titration of PIP-THQ (Fig. 2) was performed on an EnSpire 2300 Multimode plate reader (Perkin-Elmer, Singapore) in a black polypropylene 384-well plate (Cat. No. 781209, Greiner Bio-One, Frickenhausen, Germany). Fluorescence emission spectra of the fluorophore amine-THQ were acquired at 400 nm excitation during HPLC analysis. Extinction coefficients were determined in potassium phosphate buffer (0.1 M in MQW, pH 7) at 25 °C on an Agilent 8453 UV–VIS spectrophotometer (Hewlett-Packard).

2.3. Small-scale reactions of amino acids and amines

Amino acids (2 mM) were incubated with amines (1 M) in 100–200 μL MQW in 1.5 mL Eppendorf tubes heated in Thermomixer Comfort (Eppendorf) at 65 °C for 20 min, then immediately cooled on

Please cite this article as: P. Tomek, et al., Formation of fluorophores from the kynurenine pathway metabolite *N*-formylkynurenine and cyclic amines involves transamidation and carbon–carbon bond..., Biochim. Biophys. Acta (2015), http://dx.doi.org/10.1016/j.bbagen.2015.04.007

ice and analysed on LC-MS (single quadrupole). Peak areas (mV s) of corresponding adducts were quantified from 254 nm (amine-KYN and amine-NFK) and 400 nm (amine-THQ) chromatograms. Amine-amino acid adducts were identified in chromatograms by their a) predicted molecular ions in positive and negative mass spectra and b) virtually identical absorption spectra to those of a parent amino acids KYN and NFK. Amine-THQ adducts (fluorophores) were further validated from fluorescence chromatograms. Since amine-NFK and amine-KYN were incompletely separated, the double peak in chromatograms was split at the trough as depicted on Fig. 3a (dashed line) to allow quantification. Aliquots (10–20 μL) for each time point during reaction progress experiments (Fig. 4) were taken from the same tube and immediately chilled on ice prior to HPLC analysis.

2.4. Compound synthesis and characterisation

The isolation procedures described below are a result of optimisations. HPLC chromatograms of isolated compounds can be found in Fig. S.1. The yields are calculated based on 62% purity of DL-KYN.

2.4.1. 2-Amino-4-(2-formamidophenyl)-4-oxobutanoic acid (NFK)

Acetic anhydride (0.24 mL, 2.54 mmol) was added to formic acid (0.48 mL, 12.7 mmol) and the solution was warmed at 50–55 °C for 15 min, then cooled to room temperature. A solution of DL-kynurenine (0.50 g, 2.40 mmol) in formic acid (14 mL) was added and the mixture was stirred at room temperature for 2 h. Ether was added to precipitate out the product, which was washed further with ether and dried *in vacuo* to give NFK as a hygroscopic tan powder (0.38 g, ~100%). Purity was 96%. ^{1}H NMR δ (400 MHz, D_2O, 298 K) (rotamers about the formanilide group evident) 8.90 (s, 0.35H, CHO, rotamer A), 8.40 (s, 0.65H, CHO, rotamer B), 8.20 (d, J = 8.2 Hz, 0.65H, H-6′, rotamer B), 8.09 (d, J = 8.2 Hz, 0.35H, H-6′, rotamer B), 8.05 (d, J = 8.0 Hz, 0.65H, H-3′, rotamer B), 7.71 (dd, J = 8.2, 7.7 Hz, 1H, H-5′, rotamers A and B), 7.60 (d, J = 8.0 Hz, 0.35H, H-3′, rotamer A), 7.41 (dd, J = 8.0, 7.7 Hz, 1H, H-4′, rotamers A and B), 4.20 (t, J = 4.9 Hz, 1H, H-2), 3.80 (d, J = 4.9 Hz, 2H, H-3). MS *m/z* 237.0 (100%, $[M + H]^+$). HRMS *m/z* calcd for $C_{11}H_{13}N_2O_4$ 237.0870, found 237.0864 $[M + H]^+$. $\lambda_{max}(H_2O)$/nm 261 and 322 (ε/M^{-1} cm^{-1} 6289 and 1936), lit., [27] nm 260 and 321 (ε/M^{-1} cm^{-1} 10,980 and 3750). Other authors reported $\lambda_{max}(H_2O)$/nm 321 (ε/M^{-1} cm^{-1} 3152) from commercially available product [28]. We have previously isolated a small quantity of pure NFK from enzymatically catalysed oxidative cleavage of TRP [25] and obtained $\lambda_{max}(H_2O)$/nm 323 (ε/M^{-1} cm^{-1} 3066).

2.4.2. [^{13}C-formyl] labelled NFK

This material was prepared from DL-kynurenine as described above for NFK, except that the acetic anhydride was added to [^{13}C]-HCOOH in the first step. The kynurenine was added to the resulting solution, dissolved in normal formic acid. The ^{1}H NMR spectrum of the product was the same as that described above for NFK, except that there were two additional doublets present from the rotamers of the ^{13}C-labelled formyl group, due to ^{1}H–^{13}C coupling, at δ 8.86 (d, $J_{H\text{-}C}$ = 234.3 Hz, CHO, rotamer A) and 8.40 (d, $J_{H\text{-}C}$ = 203.1 Hz, CHO, rotamer B). ^{1}H NMR analysis indicated the sample to consist of an approximately 3:2 mixture of ^{13}C:^{12}C-labelled NFK. MS *m/z* 237.0 (64.88%, [^{12}C M + H]$^+$), 238.0 (100%, [^{13}C M + H]$^+$).

2.4.3. 2-(1-formylpiperidin-2-yl)-4-oxo-1,2,3,4-tetrahydroquinoline-2-carboxylic acid (PIP-THQ)

NFK (1.84 g, 7.8 mmol) was incubated with PIP (45.5 mL, 460 mmol) in 368 mL MQW at 60 °C for 20 min. The reaction was cooled on ice, evaporated to dryness and subsequently redissolved in 0.04% (*v/v*) trifluoroacetic acid (TFA) in MQW (15 mL). This solution was loaded onto a Strata C18-E cartridge (5 g/20 mL, Phenomenex) preconditioned with 70 mL MeCN and equilibrated with 70 mL of 0.04% (*v/v*) TFA in MQW. The column was eluted with mixtures of MeCN/0.04% TFA on a vacuum manifold and fractions (10 mL) were analysed on HPLC. PIP-THQ fractions were pooled, evaporated, resuspended in sodium hydroxide (143 mM, 3.5 mL) and evaporated again. The sample was resuspended in MQW (0.5 mL), loaded onto a C18 cartridge (1 g/6 mL, Varian) and eluted successively with MQW, 50% MeCN in MQW and 100% MeCN. MeCN eluates were pooled, evaporated and dried at high vacuum to yield PIP-THQ as a yellow powder after freeze-drying (17.6 mg, 0.96%). Purity was 94%. The product was a 1:1 mixture of diastereomers. ^{1}H NMR δ (400 MHz, D_2O, 298 K) 8.06 (s. 0.5H, CHO), 8.02 (s, 0.5H, CHO), 7.50–7.46 (m, 2H, H-5,7), 6.92 (dd, J = 8.2, 0.8 Hz, 1H, H-8), 6.80–6.74 (m, 1H, H-6), 4.45 (br d, J = 6.5 Hz, 0.5H, H-2′), 4.01 (dd, J = 14.6, 4.4 Hz, 0.5H, H-6′), 3.80 (dd, J = 6.8, 3.2 Hz, 0.5H, H-2′), 3.50 (dd, J = 13.1, 4.6 Hz, 0.5H, H-6′), 3.40 (m, 0.5H, H-6′), 2.71 (m, 0.5H, H-6′), 2.52 (2xd, J = 15.1 Hz, 1H, H-3), 2.49 (2xd, J = 15.1 Hz, 1H, H-3), 1.59–1.20 (m, 6H, H-3′, 4′ 5′). ^{13}C NMR spectrum-see Table S.1. MS *m/z* 303.1 (90.94%, $[M + H]^+$), 112.1 (100%, *N*-formyl-2,3,4,5-tetrahydropyridin-1-ium), 627.1 (40.22%, $[2 M + Na]^+$). HRMS *m/z* calcd for $C_{16}H_{18}N_2NaO_4$ 325.1159, found 325.1162 $[M + Na]^+$. $\lambda_{max}(H_2O)$/nm 400 (ε/M^{-1} cm^{-1} 2136).

2.4.4. [^{13}C-formyl] labelled PIP-THQ

[^{13}C-formyl]-NFK (2.56 mg, 0.011 mmol) was incubated with PIP (0.3 mL, 3.04 mmol) in MQW (3 mL) at 65 °C for 20 min. The reaction was cooled on ice, acidified to ~pH 1 with HCl and extracted twice with ethyl acetate (EtOAc). The EtOAc extract was washed twice with saturated sodium chloride solution containing 0.3% (*v/v*) HCl, evaporated and resuspended in methanol (MeOH) prior to MS analysis.

2.4.5. 2-(1-formyl-5-methylpiperidin-2-yl)-4-oxo-1,2,3,4-tetrahydroquinoline-2-carboxylic acid (3-MePIP-THQ)

NFK (80.24 mg, 7.8 mmol) was incubated with 3-methylpiperidine (3-MePIP; 2.0 mL, 17.04 mmol) in MQW (17 mL) at 65 °C for 30 min. The reaction was evaporated and subsequently redissolved in 15 mL MQW, acidified to ~pH 1 with HCl and extracted with EtOAc. The dried extract was dissolved in 3 mL MeOH:MeCN (5:1) and diluted with 30 mL MQW. The extract was fractionated on a Strata C18-E cartridge (5 g/20 mL, Phenomenex) using mixtures of MeCN/MQW containing 0.04% (*v/v*) TFA. Fractions containing 3-MePIP-THQ were pooled, evaporated and dissolved in MQW, adjusted to ~pH 8 by sodium hydroxide and mixed with ammonium bicarbonate buffer (0.02 M final concentration, pH 8). 3-MePIP-THQ was subsequently purified on a Strata C18-E cartridge (2 g/12 mL, Phenomenex) and eluted by mixtures of MeCN/MQW containing ammonium bicarbonate (0.02 M, pH 8). Eluted 3-MePIP-THQ was acidified to ~pH 1 and extracted with EtOAc, washed with saturated sodium chloride solution and dried over sodium sulphate. Subsequent evaporation and drying at high vacuum afforded 3-MePIP-THQ as a yellow powder (1.47 mg, 1.83%). Purity was 94%. The product was a mixture of diastereomers. ^{1}H NMR δ (400 MHz, $CDCl_3$, 298 K) 8.21 (s. 0.5H, CHO), 8.03 (s, 0.5H, CHO), 7.64 (dd, J = 8.4, 8.2 Hz, 1H, ArH), 7.53 (ddd, J = 8.2, 8.2, 1.2 Hz, 0.5H, ArH), 7.48 (ddd, J = 8.2, 8.2, 1.2 Hz, 0.5H, ArH), 7.02 (d, J = 8.2 Hz, 0.5H, ArH), 6.96–6.84 (m, 1.5H, ArH), 6.48 (br s, 0.5H, NH), 6.24 (br s, 0.5H, NH), 4.88 (br d, J = 4.1 Hz, 0.5H, CHN), 4.24 (dd, J = 13.4, 3.4 Hz, 0.5H, C*H*HN), 3.97 (d, J = 6.6 Hz, 0.5H, CHN), 3.23 (dd, J = 13.8, 4.1 Hz, 0.5H, C*H*HN), 2.97 (d, J = 16.3Hz, 0.5H, C*H*HCO), 2.87 (dd, J = 11.3, 11.3Hz, 0.5H, CH*H*N), 2.69 (d, J = 16.0Hz, 0.5H, C*H*HCO), 2.61 (dd, J = 12.3, 12.3 Hz, 0.5H, CH*H*N), 2.48 (d, J = 16.3 Hz, 0.5H, CH*H*CO), 2.23 (d, J = 16.0 Hz, 0.5H, CH*H*CO), 1.77–1.28 (m, CH_2), 0.94 (d, J = 6.4 Hz, 1.5H, CH_3), 0.90 (d, J = 6.0 Hz, 1.5H, CH_3). MS *m/z* 317.1 (98.18%, $[M + H]^+$), 126.1 (100%, *N*-formyl-3-methyl-2,3,4,5-tetrahydropyridin-1-ium), 339.0 (60.60%, $[M + Na]^+$), 655.2 (32.11%, $[2 M + Na]^+$). $\lambda_{max}(H_2O)$/nm 402 (ε/M^{-1} cm^{-1} 2431).

Please cite this article as: P. Tomek, et al., Formation of fluorophores from the kynurenine pathway metabolite *N*-formylkynurenine and cyclic amines involves transamidation and carbon–carbon bond..., Biochim. Biophys. Acta (2015), http://dx.doi.org/10.1016/j.bbagen.2015.04.007

2.4.6. 4-(2-aminophenyl)-4-oxo-2-(piperidin-1-yl)butanoic acid (PIP-KYN)

KYN (16.64 mg, 0.08 mmol) was incubated with PIP (0.395 mL, 4 mmol) in MQW (4 mL) at 80 °C for 30 min. The reaction was evaporated, redissolved in MQW and acidified to pH ~4 with TFA. Purification was carried out on a C18-E cartridge (2 g/12 mL, Phenomenex) using MeCN/MQW mixtures containing 0.016% (*v*/*v*) TFA. Freeze-drying of purified PIP-KYN yielded a brown powder (4.7 mg, 45%). Purity was 95%. ^{1}H NMR δ (400 MHz, D_2O, 303 K) 7.99 (dd, J = 8.1, 1.3 Hz, 1H, H-6′), 7.57 (ddd, J = 7.2, 7.1, 1.2 Hz, 1H, H-4′), 7.25 (ddd, J = 8.1, 7.2, 1.2 Hz, 1H, H-5′), 7.19 (dd, J = 7.1, 1.2 Hz, H-3′), 4.35 (dd, J = 7.0, 4.4 Hz, 1H, H-2), 3.85 (dd, J = 18.2, 7.0 Hz, 1H, H-3), 3.72 (dd, J = 18.2, 4.4 Hz, 1H, H-3), 3.51 (br d, J = 11.7 Hz, 1H, C*H*HN), 3.40 (br d, J = 11.7 Hz, 1H, CH*H*N), 3.13–2.95 (m, 2H, CH_2N), 1.93–1.68 (m, 5H, CH_2), 1.47–1.34 (m, 1H, CH). MS *m*/*z* 277.2 (100%, $[M + H]^+$). HRMS *m*/*z* calcd for $C_{15}H_{21}N_2O_3$ 277.1547, found 277.1538 $[M + H]^+$. $\lambda_{max}(H_2O)$/nm 259 and 364 (ε/M^{-1} cm^{-1} 7213 and 4010).

2.4.7. 4-(2-aminophenyl)-4-oxo-2-butenoic acid (KYN-CKA)

KYN (58.24 mg, 0.28 mmol) was incubated with sodium hydroxide (7 mg, 0.175 mmol) in MQW (8.75 mL, pH ~12) at 80 °C for 9 min, immediately cooled on ice and brought to pH ~2 using HCl. This solution was extracted three times with EtOAc, and the organic layer was pooled and washed four times with saturated NaCl. Subsequent evaporation and drying at high vacuum afforded KYN-CKA as a bright orange powder (9 mg, 24%). Purity was 96%. ^{1}H NMR δ (400 MHz, DMSO-d_6, 298 K) 7.74 (dd, J = 8.2, 1.5 Hz, 1H, H-6′), 7.53 (d, J = 15.7 Hz, 1H, H-3), 7.32 (ddd, J = 7.1, 7.2, 1.5 Hz, 1H, H-4′), 6.78 (dd, J = 8.7, 0.9 Hz, 1H, H-3′), 6.70 (ddd, J = 8.2, 7.1, 0.9 Hz, 1H, H-5′), 6.62 (d, J = 15.7 Hz, 1H, H-2). MS *m*/*z* 192.0 (100%, $[M + H]^+$), 213.9 (85.37%, $[M + Na]^+$), 189.9 (100%, $[M-H]^-$). HRMS *m*/*z* calcd for $C_{10}H_9NNaO_3$ 214.0475, found 214.0466 $[M + Na]^+$. $\lambda_{max}(H_2O)$/nm 392 (ε/M^{-1} cm^{-1} 4205). λ_{max}(EtOH)/nm 411 (ε/M^{-1} cm^{-1} 4493).

2.4.8. 4-(2-Formamidophenyl)-4-oxo-2-butenoic acid (NFK-CKA)

NFK (65.7 mg, 0.316 mmol) was heated with PIP (1.78 mL, 18 mmol) in 81% (*v*/*v*) 2-propanol in MQW (20 mL) at 52 °C for 55 min. Subsequently, the reaction was cooled on ice and rapidly neutralised to ~pH 7 by HCl and evaporated to dryness. The residue was dissolved in ammonium bicarbonate (0.05 M, pH 7), loaded onto a Strata C18-E cartridge (5 g/20 mL) and eluted using MeCN/MQW mixtures containing ammonium bicarbonate (0.03 M, pH 7). Fractions containing NFK-CKA adduct were put into a freezer (−20 °C). Next day, isolated NFK-CKA was left at room temperature for >3 h, acidified with HCl to pH 2 and extracted with 2 volumes of EtOAc. The EtOAc extract was washed with saturated sodium chloride solution and evaporated. Dry material was resuspended in MeOH, sonicated, and centrifuged for 5 min at 14,000 *g*. The supernatant, which contained impurities and a small amount of NFK-CKA was removed and the pellet was dried at high vacuum to afford NFK-CKA as a pale yellow powder (12.55 mg, 19.1%). Compound was unstable in MS but appeared pure from NMR and HPLC. Purity was 98%. ^{1}H NMR δ (400 MHz, DMSO-d_6,298 K) 13.20 (br, 1H, COOH), 10.82 (s, 1H, N*H*CHO), 8.38 (s, 1H, CHO), 8.14 (d, J = 7.8 Hz, 1H, H-6′), 7.87 (d, J = 7.4 Hz, 1H, H-3′), 7.64 (dd, J = 7.4, 7.3 Hz, 1H, H-4′), 7.62 (d, J = 15.6 Hz, 1H, H-3), 7.29 (dd, J = 7.8, 7.3Hz, 1H, H-5′), 6.56 (d, J = 15.6 Hz, 1H, H-2). HRMS *m*/*z* calcd for $C_{11}H_9NNaO_4$ 242.0424, found 242.0425 $[M + Na]^+$. $\lambda_{max}(H_2O)$/nm 322 (ε/M^{-1} cm^{-1} 1584). λ_{max}(THF)/nm 285 and 350 (ε/M^{-1} cm^{-1} 4355 and 2596).

3. Results and discussion

3.1. Structure and properties of PIP-THQ fluorophore

3.1.1. NMR studies

NFK was synthesised by formylation of KYN using a modification of a published method [27]. It was then reacted with an excess of PIP at 60 °C under aqueous conditions, and the fluorophore was purified using reversed phase preparative chromatography (see Section 2.4.3). The product displayed a molecular ion adduct $[M + H]^+$ at *m*/*z* 303.1 and sodium adduct $[M + Na]^+$at 325.1159 amu on low resolution triple quadrupole mass spectrometry and high resolution time-off-flight mass spectrometry, respectively, consistent with a molecular formula $C_{16}H_{18}N_2O_4$ and molecular weight 302 Da. It was clear from both the ^{1}H and ^{13}C NMR spectra that the sample was a 1:1 mixture of isomers, with most of the resonances being doubled up (Fig. S.2a,b). The four aromatic resonances of the starting NFK were still present, and resonances characteristic of a PIP group were clearly evident at δ 4.4–2.7 ppm (CH—N) and δ 1.8–1.3 ppm (CH_2CH_2). Singlets at δ 8.06 and 8.02 ppm were consistent with the presence of a formyl group. Particularly diagnostic were resonances resulting from two overlapping AB spin systems centred at around 2.5 ppm, each with a large coupling constant of approximately 15 Hz. This indicates the presence of an isolated CH_2 group, probably in a ring system. Two-dimensional NMR studies (Fig. S.3–S.7) were used to identify coupled proton systems and to correlate proton and carbon resonances (Table S.1). From these it was evident that there were only three protons adjacent to the nitrogen atom of the PIP, with two of these displaying geminal coupling to each other. The remaining proton did not display geminal coupling, and appeared as a much narrower resonance. This indicates that the PIP has reacted at one of the carbon atoms adjacent to the nitrogen of the PIP, with the loss of one of its hydrogen atoms. Finally, a nitrogen NMR spectrum was obtained and indicated the presence of two nitrogen atoms in the molecule (δ 88 and 134 ppm) (Fig. S.8). Based on considerations of all this data we propose the structure shown in Scheme 2 for PIP-THQ. The product is a mixture of two racemic diastereomers at the 2 and 2′ positions (Table S.1). The placement of the formyl group on the PIP nitrogen and not the nitrogen of the quinolone ring was based on the NOESY spectrum, which suggested that it was close to the PIP ring protons, although the correlation peaks were not strong (Fig. S.7).

3.1.2. MS fragmentation studies (confirming position of the formyl group on PIP-THQ)

To confirm the position of the formyl group in the structure of PIP-THQ, mass fragmentation studies of the compound were conducted (Fig. 1). The fragmentation spectrum of [^{12}C-formyl]-PIP-THQ (*m*/*z* 303.1) shows a prominent ion at *m*/*z* 112.2 likely corresponding to the *N*-formyl-2,3,4,5-tetrahydropyridin-1-ium fragment (Fig. 1a). Further fragmentation of this ion provided *m*/*z* 84.1, indicating a loss of the formyl group (Δ *m*/*z* 28), and *m*/*z* 56.1, 42.1 and 28.1 (Δ *m*/*z* 14) typical for PIP fragmentation (Fig. 1b) [29]. To confirm that *m*/*z* 112.2 is indeed *N*-formyl-2,3,4,5-tetrahydropyridin-1-ium, we synthesised NFK using ^{13}C labelled formic acid and reacted it with PIP. This yielded a mixture of [^{13}C-formyl]-PIP-THQ and [^{12}C-formyl]-PIP-THQ in a ratio of 1.73:1 according to MS. Fragmentation of [^{13}C-formyl]-PIP-THQ is expected to yield M + 1 ion (*m*/*z* 113), and indeed the fragmentation spectrum of [^{13}C-formyl]-PIP-THQ (*m*/*z* 304.3) shows a dominant ion at *m*/*z* 113.1 (Fig. 1c), consistent with the formyl group in PIP-THQ being attached to PIP. Other ions produced were the same as those observed in the fragmentation spectrum of [^{12}C-formyl]-PIP-THQ, consistent with their formation following loss of the labelled formyl group (Fig. 1b,d).

3.1.3. Fluorescence titration and absorption spectrum of PIP-THQ

The fluorescence titration of PIP-THQ showed that pH between 3 and 11.5 did not affect PIP-THQ fluorescence intensity but extremely acidic (<1) or basic (>13) pH destroys the signal (Fig. 2). The decrease in fluorescence of PIP-THQ is likely caused either by ionisation of the quinolone nitrogen or carboxylic acid groups in PIP-THQ (pKa 1.78 and 12.56, respectively) or decomposition at pH extremes. The absorption spectrum of PIP-THQ shows distinct bands at 400 nm and 235 nm, and a shoulder at 260 nm (see Fig. 3a—inset), and differs to those of previously reported KYN-related compounds.

Please cite this article as: P. Tomek, et al., Formation of fluorophores from the kynurenine pathway metabolite *N*-formylkynurenine and cyclic amines involves transamidation and carbon–carbon bond..., Biochim. Biophys. Acta (2015), http://dx.doi.org/10.1016/j.bbagen.2015.04.007

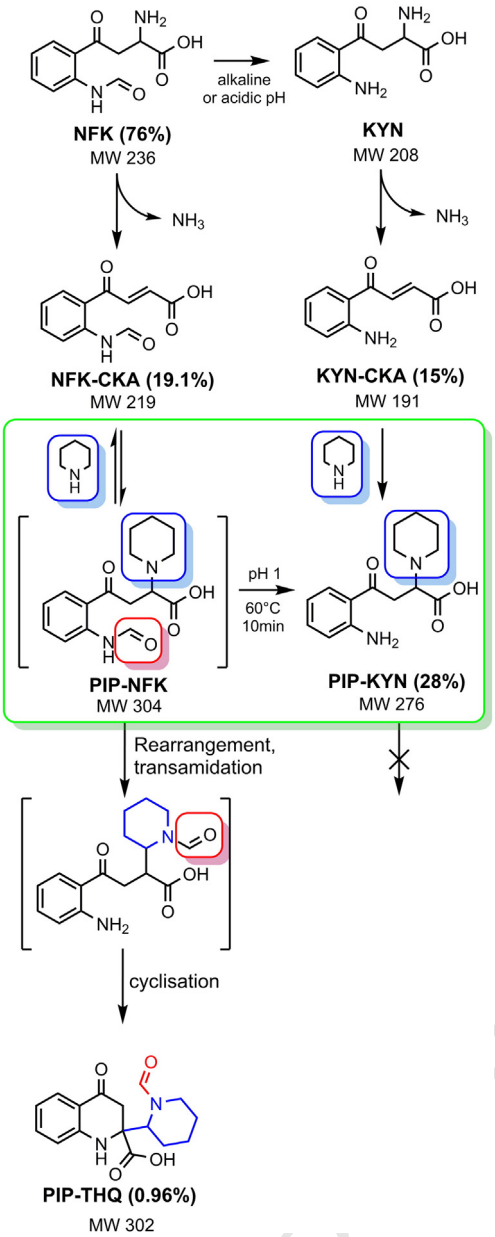

Scheme 2. Proposed pathway of NFK and KYN reactions with PIP. Step d) is not based on experimental observation. Note that PIP-KYN does not undergo any further modification when incubated with PIP. Percent yield of purified solid is indicated in parentheses.

3.2. Reaction pathway leading to the formation of PIP-THQ

Considering that PIP-THQ is produced in a moderately heated aqueous reaction with no obvious catalysts, the *N*-formylation and 2-substitution of PIP to form PIP-THQ raise an intriguing question as to the reaction mechanism involved. The UV trace from the LC-MS chromatogram of the reaction products of NFK (2 mM) and PIP (1 M) at pH 12.56 shows a large number of compounds and some were identified (Fig. 3a). The most intense peaks correspond to the PIP-THQ fluorophore eluting at R_t 9.6 min. Molecular ions $[M + H]^+$ at *m/z* 305.2 and *m/z* 277.4 coeluting at R_t 5.7 and 5.9 min (peak area ratio 1:3.4) observed in the spectrum were tentatively assigned to PIP-NFK and PIP-KYN, respectively, whilst KYN eluted at R_t 2.8 min. KYN is a substantial product of the PIP and NFK reaction and could potentially be the intermediate for fluorophore formation. However, only *m/z* 277.4 and KYN were observed in the chromatogram from the reaction of KYN and PIP (Fig. 3b). The product in the *m/z* 277.4 peak was isolated (see Section 2.4.6) and confirmed to be PIP-KYN (Scheme 2). The results suggest the formyl group is necessary for fluorophore formation, and KYN or its adduct PIP-KYN appear not to be intermediates in this process.

The unsaturated amino acid KYN-CKA has been shown to form adducts with nucleophilic protein residues and glutathione [6,10], therefore we investigated the reaction of 2 mM KYN-CKA or NFK-CKA with 1 M PIP heated at 65 °C for 20 min. The reaction of KYN-CKA and PIP showed only one dominant product (PIP-KYN) establishing that KYN-related analogues are not involved in fluorophore formation, and the hydrolysis of NFK into KYN on reaction with PIP is only a side reaction. On the other hand, reaction of NFK-CKA and PIP gave a comparable chromatogram as in Fig. 3a, consistent with deamination of NFK as a first step in fluorophore formation. When an aliquot of NFK-CKA dissolved in DMSO was mixed with PIP (1 M) at room temperature, the product corresponding to PIP-NFK (MW 304 Da, absorption spectrum comparable to NFK) was formed rapidly at ~80% purity. This strongly indicated that the formation of PIP-NFK adduct is the second step in the fluorophore formation from PIP (Scheme 2). Unfortunately, PIP-NFK could not be isolated for structural studies because it decomposed back to NFK-CKA during purification, suggesting that the reaction is reversible favouring NFK-CKA formation in the absence of PIP. However, PIP-NFK converted to PIP-KYN when heated at 60 °C for 10 min at pH 1 (Scheme 2) lending support to our proposed structure of PIP-NFK.

No reaction products were observed when TRP was heated with PIP at 65 °C for 20 min, indicating that the γ-keto group on the amino acid chain of KYN and NFK is critical for the addition of the amine.

During our studies, we noticed that >80% 2-propanol or DMSO in the reaction of NFK and PIP or NFK-CKA and PIP suppressed the formation of fluorophore PIP-THQ and PIP-KYN but not the PIP-NFK intermediate. This suggests that the conversion of PIP-NFK to the fluorophore PIP-THQ requires a high content of water.

3.3. Rate of formation and consumption of PIP-NFK and PIP-KYN and PIP-THQ

The kinetics of PIP-NFK formation is very fast compared to that of PIP-KYN formation (Fig. 4). When NFK (2 mM) was incubated with PIP (1 M) in MQW at 65 °C, the maximal amount of PIP-NFK was formed after 3 min and then decreased exponentially (Fig. 4a). In contrast, a 30 min incubation of KYN (5 mM) and PIP (1 M) at 80 °C is necessary to reach maximal formation of PIP-KYN (Fig. 4b). Rates of PIP-KYN formation ($k_{obs} = 8.2 \times 10^{-2}$ min^{-1}) and PIP-NFK consumption ($k_{obs} = 4.5 \times 10^{-2}$ min^{-1}) are comparable. As expected, KYN decomposes at about 10-fold slower rate ($k_{obs} = 2.9 \times 10^{-2}$ min^{-1}) than NFK ($k_{obs} = 3.4 \times 10^{-1}$ min^{-1}) when incubated with PIP, consistent with the higher reactivity of NFK to KYN. Whilst PIP-NFK decreases at a nearly linear rate, PIP-THQ forms exponentially ($k_{obs} = 1.3 \times 10^{-1}$ min^{-1}) and reaches a plateau before PIP-NFK is depleted. This suggests two things. Firstly, PIP-THQ is decomposing as the reaction progresses. Secondly, PIP-THQ is not formed directly from PIP-NFK. The missing step is likely a rearrangement and transamidation (Scheme 2).

Whilst the optimal reaction temperature and time for maximum formation of PIP-THQ are 65 °C for 20 min, we also observed that PIP-THQ could form at 55 °C, although at 3× slower rate [25] indicating that the higher temperature (65 °C) is not essential for the PIP-THQ formation.

3.4. Effect of PIP and NFK concentration on the formation of fluorophore PIP-THQ

The effect of varying concentrations of PIP on fluorophore formation was investigated. When a fixed concentration of PIP (1 M) was incubated with different concentrations of NFK (0.5–9 mM), PIP-THQ formation was initially nonlinear in relationship to NFK concentration and reached

Please cite this article as: P. Tomek, et al., Formation of fluorophores from the kynurenine pathway metabolite *N*-formylkynurenine and cyclic amines involves transamidation and carbon–carbon bond..., Biochim. Biophys. Acta (2015), http://dx.doi.org/10.1016/j.bbagen.2015.04.007

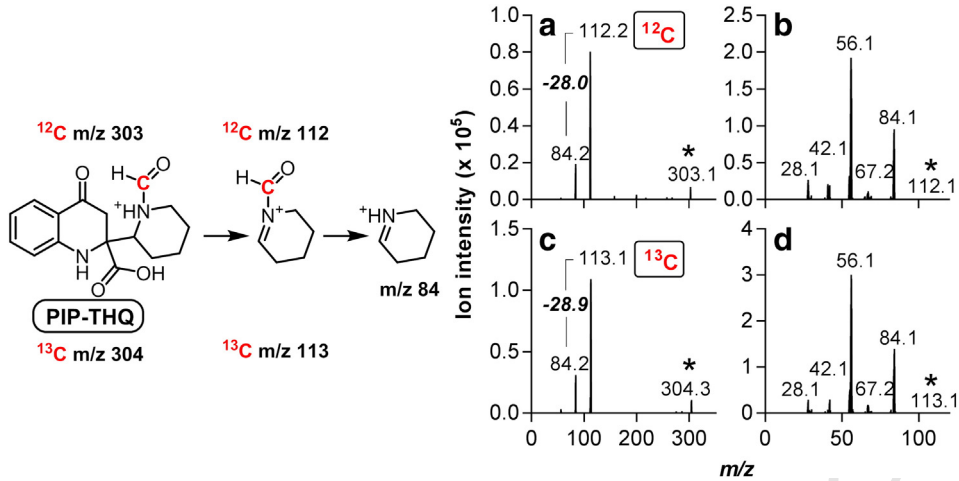

Fig. 1. Mass fragmentation of PIP-THQ isotopes in positive electrospray ionisation mode and triple quadrupole. Panel shows fragmentation spectra of ion a) *m/z* 304.3 ([^{13}C-formyl] PIP-THQ), b) *m/z* 113.1, c) *m/z* 303.1 ([^{12}C-formyl] PIP-THQ) and d) *m/z* 112.1. Voltage applied to collision cell was 10 V (a,c) and 20 V (b,d), respectively. Asterisk marks the ion being fragmented.

a plateau at 9 mM NFK (Fig. 5a). When the concentration of NFK was kept constant (2 mM) and reacted with varying concentrations of PIP (0.4, 1 and 3 M) (Fig. 5b), PIP-THQ formation at both 3 M and 0.4 M PIP was approximately half of that formed at 1 M PIP. The large molar excess (~500-fold) of PIP to NFK is necessary for efficient fluorophore formation however, concentrations of PIP higher than 1 M appear to decrease PIP-THQ formation possibly due to decomposition caused by high pH.

In contrast, the reaction of KYN and PIP does not require a high molar excess of PIP. When KYN (20 mM) was heated at 80 °C for 10 min with either a 50-fold (1 M) or 10-fold (0.2 M) excess of PIP, the yield of PIP-KYN by HPLC was comparable.

3.5. Formation of fluorophores from amines other than PIP

3.5.1. Cyclic amines

We compared fluorophore formation when NFK was reacted with 5- or 7-membered cyclic amines to that with 6-membered ring PIP. Fluorophore formation with 5-membered ring pyrrolidine (PYR), or with 7-membered ring azepane (AZP), was decreased 12% and 10% respectively, compared to PIP (Table 1). The mass and R_t of the fluorophores AZP-THQ (MW 316, R_t 10.7 min) and PYR-THQ (MW 288, R_t 8 min) were as expected in relation to the mass of the ring (Table 1). The fragmentation pattern of PYR-THQ resembled that of PIP-THQ indicating that the amine ring was similarly formylated and connected (Fig. S.9a). This showed that the fluorophore formation is not significantly affected by the size of the amine ring.

3.5.2. Monomethyl-substituted PIP and acyclic amines

Fluorophore formation from the reaction of NFK with isomeric methyl substituted PIPs was investigated (Table 1). When the methyl-substituent was located on the nitrogen of PIP (NMePIP), the mass and R_t of the formed fluorophore (NMePIP-THQ) were identical to that of PIP-THQ (MW 302, R_t 9.5 min), but 2.5-fold lower yields were obtained. A similar pattern was also observed comparing fluorophore formation between PYR and NMePYR. This indicates that the *N*-methyl group of the tertiary amine had to undergo demethylation. Much lower yields of fluorophore were obtained using 2-methylpiperidine (2-MePIP), cis-2,6-dimethylpiperidine (DMP) and 2,2,6,6-tetramethylpiperidine (TMP) (4%, 3% and 0%, respectively, compared to PIP). Furthermore, the mass of the fluorophore DMP-THQ (MW 316) formed from DMP was identical to fluorophores formed from monomethylated amines (3-MePIP-THQ and 4-MePIP-THQ) (Table 1). DMP forms both amine-KYN and amine-NFK adducts with slight decreases in efficiency compared to PIP (29% and 36% respectively). This suggested that the commercial DMP used in the study (Sigma-Aldrich,

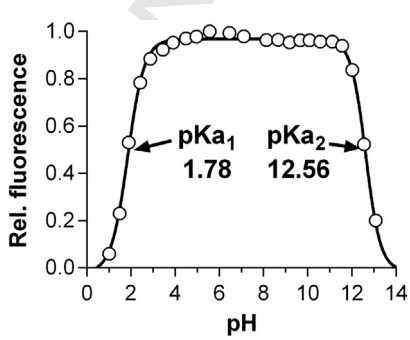

Fig. 2. Fluorescence titration of 15 μM PIP-THQ measured in 0.1 M KCl at 25 °C. pH was adjusted with KOH and HCl. Excitation and emission wavelengths were 400 and 500 nm, respectively. Data were fitted with bell shaped curve which afforded values at inflection points.

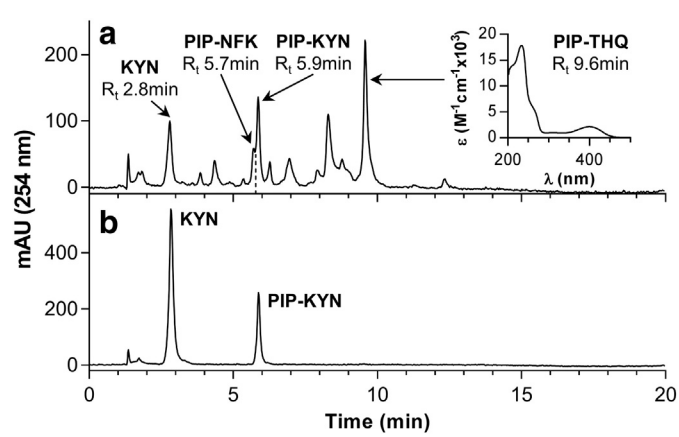

Fig. 3. HPLC chromatogram of reaction of a) NFK (2 mM) or b) KYN (2 mM) with PIP (1 M) incubated at 65 °C for 20 min, cooled on ice and analysed on HPLC-MS. Detection wavelength was 254 nm. Compound name and retention time (R_t) are indicated. Absorption spectrum of PIP-THQ is shown in the inset. Dashed line denotes the separation of PIP-KYN and PIP-NFK peaks for quantification purposes.

Please cite this article as: P. Tomek, et al., Formation of fluorophores from the kynurenine pathway metabolite *N*-formylkynurenine and cyclic amines involves transamidation and carbon–carbon bond..., Biochim. Biophys. Acta (2015), http://dx.doi.org/10.1016/j.bbagen.2015.04.007

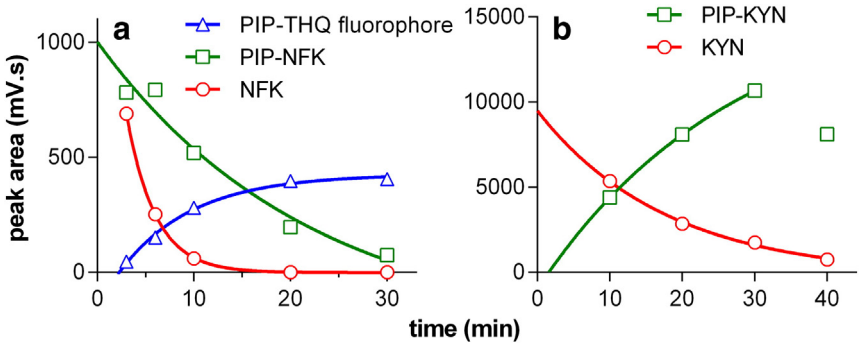

Fig. 4. Reaction progress of a) 2 mM NFK and 1 M PIP at 65 °C and b) 5 mM KYN and 1 M PIP at 80 °C. Each time point aliquot was analysed by HPLC and peak areas of corresponding compounds were quantified from 400 nm (PIP-THQ), 360 nm (PIP-KYN and KYN), and 325 nm (PIP-NFK and NFK) chromatograms. Data points were fitted with one-phase exponential curves. Data point of PIP-KYN at 40 min in panel b) was not included in the fit.

98%) might have been contaminated with isomers of monomethyl PIP. Indeed, comparing ^{13}C NMR spectra of DMP, 2-Me, 3-Me and 4-Me PIP showed that DMP contains about 1% of 3-MePIP but other impurities were also present. In Section 3.4, we showed that formation of PIP-KYN adducts does not require a high molar excess of PIP, in contrast to formation of fluorophores. This strongly indicates that the adducts observed in the reaction of DMP and NFK are 3-MePIP adducts and that DMP itself is only marginally reactive. It also corroborates the requirement for a high molar excess of PIP (and most likely also other amines) to NFK for the fluorophore formation.

Formation of the amine-THQ fluorophore from 3-MePIP and 4-MePIP was increased 1.84-fold and 1.38-fold respectively compared to PIP. Acyclic amines diethylamine (DEA) and dipropylamine (DPA) formed THQ products in much lower quantities than with PIP.

The fluorescence emission maxima of PIP-THQ and the other amine-THQ fluorophores were comparable (Table 1), showing that the structure of amine has negligible effect on the electronic properties of the fluorophores. We purified 3-MePIP-THQ and confirmed using mass fragmentation (Fig. S.9b) and NMR (Fig. S.10–S.12), that it was indeed an analogue of PIP-THQ, differing only in the attached amine. Moreover, comparable extinction coefficients of 3-MePIP-THQ ($\varepsilon_{402} = 2431\ M^{-1}\ cm^{-1}$) and PIP-THQ ($\varepsilon_{400} = 2136\ M^{-1}\ cm^{-1}$) strongly indicates the yields in Table 1 obtained from peak areas of 400 nm chromatogram are genuine, and not a result of different extinction coefficients.

3.5.3. Summary of reactions of amines with NFK

1) Cyclic amines form fluorophores more efficiently than acyclic amines of comparable size and basicity. This suggests that the rearrangement and transamidation step requires a finely tuned spatial arrangement that does not favour acyclic structures.

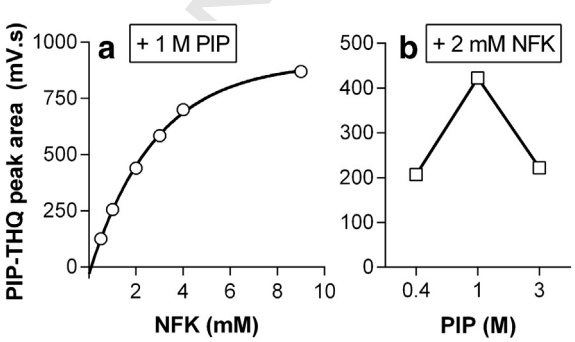

Fig. 5. Formation of PIP-THQ in reaction of a) variable NFK and 1 M PIP and b) 2 mM NFK and variable PIP. Reactions were initiated by addition of PIP into aqueous solution of NFK, incubated at 65 °C for 20 min, chilled on ice and analysed on HPLC. Peak area corresponding to PIP-THQ was quantified from 400 nm chromatogram.

2) Only cyclic amines without substitutions at both carbons adjacent to nitrogen (2- and 6-position on PIP ring) appear to be able to form fluorophores efficiently. One position next to nitrogen is required for bond formation during the rearrangement step, but why both positions next to nitrogen need to be unsubstituted is not yet clear. As suggested in point 1), a methyl group adjacent to nitrogen might sterically hinder the interaction of the formyl group with the amine nitrogen.
3) 3- and 4-methyl substituents on PIP enhance fluorophore formation.

3.6. Reactions of amines with KYN

In a final aspect of our investigations, we examined reactions of amines with KYN, an NFK analogue without the formamide group. Chromatograms of the reaction of KYN with amines showed only unreacted KYN and amine-KYN adduct(s) (Table 1). NMePIP-KYN and DMP-KYN adducts also showed a loss of the methyl substituent, similar to their respective fluorophores NMePIP-THQ and DMP-THQ formed from NFK (Table 1). 4-MePIP did not significantly increase the yield of amine-KYN adduct relative to PIP. This contrasts with the increased yields of amine-NFK and amine-THQ that were obtained in the reaction of NFK with 4-MePIP and 3-MePIP compared to PIP. Thus, a 4-methyl substituent on the PIP skeleton is favoured during fluorophore formation but has a negligible effect on amine-KYN adduct formation.

Acyclic secondary amines DEA and DPA formed DEA-KYN and DPA-KYN adducts with 86% and 39% efficiency, respectively, compared to PIP-KYN. This again contrasts with NFK reactions where the acyclic amines did not form adducts apart from small amounts of fluorophore amine-THQ. Moreover, acyclic amines DPA and DEA produced two different KYN adducts; the more abundant adduct having apparently lost one of the alkyl chains, whilst the lower yielding adduct did not. In contrast, reactions of cyclic amines produced only a single amine-KYN adduct with exception of 2-MePIP which also formed two products but with identical mass (MW 290, Table 1). The two 2-MePIP-KYN adducts are most likely diastereomers.

4. Concluding remarks

The reaction of NFK and cyclic amines generates tetrahydroquinolone-based fluorophores where the amine is *N*-formylated and attached through its 2-position. Substitutions on the 2-position of piperidine [30–34] and transamidations [35–39] in general require high temperatures or catalysts. In contrast, our newly-described reaction does not require catalysts and occurs in aqueous solution under mild conditions. Fluorophore formation is driven by a high molar excess of cyclic amine relative to NFK which provides the basic environment for initial NFK deamination and the subsequent formation of a transient adduct, PIP-NFK. This is then followed by amine-induced transamidation of the formyl group from NFK to the nitrogen of the amine, adduct rearrangement

Please cite this article as: P. Tomek, et al., Formation of fluorophores from the kynurenine pathway metabolite *N*-formylkynurenine and cyclic amines involves transamidation and carbon–carbon bond..., Biochim. Biophys. Acta (2015), http://dx.doi.org/10.1016/j.bbagen.2015.04.007

Table 1
Molecular weights (MW), retention times (R_t) and amount of amine-KYN, amine-NFK, amine-THQ adducts formed in reaction of amines with NFK (red font), and the amine-KYN adduct formed in the reaction of amines with KYN (blue font).

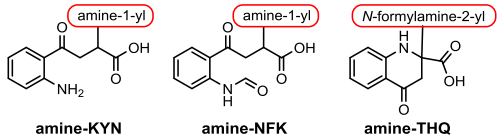

amine	amine–KYN MW (Da)	amine–KYN R_t (min)	amine–KYN Peak area (%)[b] NFK rxn[c]	amine–KYN Peak area (%)[b] KYN rxn[c]	amine–NFK MW (Da)	amine–NFK R_t (min)	amine–NFK Peak area (%)[b]	amine–THQ MW (Da)	amine–THQ R_t (min)	amine–THQ Peak area (%)[b]	λ_{em}[d] (nm)
PIP	276	5.9	100*	100*	304	5.7	100	302	9.6	100* (100%)	486
NMePIP	276	5.9	16	70	304	5.7	102	302	9.6	39	486
2–MePIP	290 290	6.3 6.8	0 48	39 17	N/O		0	316	10.6	4	N/O
3–MePIP	290	7.1	94	N/T	318	6.8	272	316	10.9	184* (190%)	485
4–MePIP	290	7.1	114	113	318	6.8	275	316	10.9	138	484
DMPe	290	7.1	71	82	318	6.8	64	316	10.9	3	484
TMP (40% 2–propanol)	N/O		0	N/T	N/O		0	N/O		0	N/O
PYR	262	4.9	190[a]	N/T	290		190[a]	288	8	88	488
NMePYR	N/O		0	N/T	N/O		0	288	8	35	486
AZP	N/O		0	N/T	N/O		0	316	10.7	90	483
DEA	236 264	4.1 5.5	0 0	59 27	N/O		0 0	290	9	10	485
DPA (40% 2–propanol)	250 292	5.2 7.8	0 0	30 9	N/O		0 0	318	11	1	483

N/O = not observed; N/T = not tested. Molecular weights were determined by presence of $[M + H]^+$ and $[M - H]^-$ ions in mass spectra of respective compounds at given retention time (R_t). Reactions of TMP and DPA were performed in 40% 2-propanol due to their poor water solubility.

[a] PYR-KYN and PYR-NFK adducts coeluted in a single peak, and the value represents their combined peak areas.

[b] Peak areas expressed relative to PIP reactions (100%) in each respective column. The percent value in parentheses denotes the yield of purified solid relative to PIP-THQ.

[c] These two columns show peak areas of amine-KYN adducts observed in reactions of NFK (NFK rxn) and KYN (KYN rxn) with amines.

[d] The fluorescence emission maximum at 400 nm excitation, acquired during HPLC analysis.

[e] The products in reaction of DMP with amino acids are probably formed from impurities in the DMP reagent.

* Asterisk denotes that the compound was purified and isolated.

and cyclisation which requires a high content of water. The sequence of the final steps is not clear, but cyclisation is likely to be a rate-limiting step as thermal decomposition of KYN to form KNY (Scheme 1) proceeds at a slow rate [8]. The formamide group of NFK is essential for fluorophore formation, and efficient fluorophore formation is limited to cyclic amines that are unsubstituted on both positions adjacent to the nitrogen of the amine.

We have demonstrated that NFK is a highly reactive TRP catabolite indicating that it could form yet to be identified biologically relevant metabolites warranting further study.

We have been using the formation of PIP-THQ fluorophore in our most current and most sensitive IDO1 enzymatic assay [25], but the studies here suggest that using 3-MePIP instead of PIP might increase the sensitivity of this assay even more. Isolation of remaining fluorophore intermediates and determination of reaction kinetics and reaction orders in future experiments would aid in identifying the final steps of this reaction mechanism.

Conflicts of interest

Authors do not have any conflicts of interest to disclose.

Transparency Document

The Transparency document associated with this article can be found, in the version.

Acknowledgements

This work was supported by grants from the Auckland Cancer Society and the University of Auckland doctoral scholarship to P.T. Q3

Appendix A. Supplementary data

Supplementary data to this article can be found online at http://dx.doi.org/10.1016/j.bbagen.2015.04.007.

References

[1] Y. Chen, G.J. Guillemin, Kynurenine pathway metabolites in humans: disease and healthy states, Int. J. Tryptophan Res. 2 (2009) 1–19.
[2] G. Costantino, New promises for manipulation of kynurenine pathway in cancer and neurological diseases, Expert Opin. Ther. Targets 13 (2009) 247–258.
[3] M. Sono, M.P. Roach, E.D. Coulter, J.H. Dawson, Heme-containing oxygenases, Chem. Rev. 96 (1996) 2841–2888.
[4] A.H. Mehler, W.E. Knox, The conversion of tryptophan to kynurenine in liver: II. The enzymatic hydrolysis of formylkynurenine, J. Biol. Chem. 187 (1950) 431–438.
[5] L.M. Taylor, J. Andrew Aquilina, J.F. Jamie, R.J.W. Truscott, UV filter instability: consequences for the human lens, Exp. Eye Res. 75 (2002) 165–175.
[6] B. Garner, D.C. Shaw, R.A. Lindner, J.A. Carver, R.J.W. Truscott, Non-oxidative modification of lens crystallins by kynurenine: a novel post-translational protein modification with possible relevance to ageing and cataract, Biochim. Biophys. Acta Protein Struct. Mol. Enzymol. 1476 (2000) 265–278.
[7] N.R. Parker, A. Korlimbinis, J.F. Jamie, M.J. Davies, R.J.W. Truscott, Reversible binding of kynurenine to lens proteins: potential protection by glutathione in young lenses, Invest. Ophthalmol. Vis. Sci. 48 (2007) 3705–3713.
[8] Y.P. Tsentalovich, O.A. Snytnikova, M.D.E. Forbes, E.I. Chernyak, S.V. Morozov, Photochemical and thermal reactivity of kynurenine, Exp. Eye Res. 83 (2006) 1439–1445.
[9] L.V. Kopylova, O.A. Snytnikova, E.I. Chernyak, S.V. Morozov, M.D.E. Forbes, Y.P. Tsentalovich, Kinetics and mechanism of thermal decomposition of kynurenines and biomolecular conjugates: ramifications for the modification of mammalian eye lens proteins, Org. Biomol. Chem. 7 (2009) 2958–2966.
[10] P.T. Yu, O.A. Snytnikova, R.Z. Sagdeev, Photochemical and thermal reactions of kynurenines, Russ. Chem. Rev. 77 (2008) 789.
[11] A.L. Mellor, D.H. Munn, IDO expression by dendritic cells: tolerance and tryptophan catabolism, Nat. Rev. Immunol. 4 (2004) 762–774.
[12] G.K. Lee, H.J. Park, M. Macleod, P. Chandler, D.H. Munn, A.L. Mellor, Tryptophan deprivation sensitizes activated T cells to apoptosis prior to cell division, Immunology 107 (2002) 452–460.
[13] F. Fallarino, U. Grohmann, S. You, B.C. McGrath, D.R. Cavener, C. Vacca, C. Orabona, R. Bianchi, M.L. Belladonna, C. Volpi, P. Santamaria, M.C. Fioretti, P. Puccetti, The combined effects of tryptophan starvation and tryptophan catabolites down-regulate T cell receptor ζ-chain and induce a regulatory phenotype in naive T cells, J. Immunol. 176 (2006) 6752–6761.
[14] Y. Suzuki, T. Suda, K. Furuhashi, M. Suzuki, M. Fujie, D. Hahimoto, Y. Nakamura, N. Inui, H. Nakamura, K. Chida, Increased serum kynurenine/tryptophan ratio correlates with disease progression in lung cancer, Lung Cancer 67 (2010) 361–365.
[15] D.H. Munn, M.D. Sharma, D. Hou, B. Baban, J.R. Lee, S.J. Antonia, J.L. Messina, P. Chandler, P.A. Koni, A.L. Mellor, Expression of indoleamine 2,3-dioxygenase by plasmacytoid dendritic cells in tumor-draining lymph nodes, J. Clin. Invest. 114 (2004) 280–290.
[16] K. Ino, N. Yoshida, H. Kajiyama, K. Shibata, E. Yamamoto, K. Kidokoro, N. Takahashi, M. Terauchi, A. Nawa, S. Nomura, T. Nagasaka, O. Takikawa, F. Kikkawa, Indoleamine 2,3-dioxygenase is a novel prognostic indicator for endometrial cancer, Br. J. Cancer 95 (2006) 1555–1561.

Please cite this article as: P. Tomek, et al., Formation of fluorophores from the kynurenine pathway metabolite *N*-formylkynurenine and cyclic amines involves transamidation and carbon–carbon bond..., Biochim. Biophys. Acta (2015), http://dx.doi.org/10.1016/j.bbagen.2015.04.007

[17] M. Hoshi, H. Ito, H. Fujigaki, M. Takemura, T. Takahashi, E. Tomita, M. Ohyama, R. Tanaka, K. Saito, M. Seishima, Indoleamine 2,3-dioxygenase is highly expressed in human adult T-cell leukemia/lymphoma and chemotherapy changes tryptophan catabolism in serum and reduced activity, Leuk. Res. 33 (2009) 39–45.
[18] C. Uyttenhove, L. Pilotte, I. Théate, V. Stroobant, D. Colau, N. Parmentier, T. Boon, B.J. Van den Eynde, Evidence for a tumoral immune resistance mechanism based on tryptophan degradation by indoleamine 2,3-dioxygenase, Nat. Med. 9 (2003) 1269–1274.
[19] E. Dolušić, R. Frédérick, Indoleamine 2,3-dioxygenase inhibitors: a patent review (2008–2012), Expert Opin. Ther. Pat. 23 (2013) 1367–1381.
[20] X. Zheng, J. Koropatnick, M. Li, X. Zhang, F. Ling, X. Ren, X. Hao, H. Sun, C. Vladau, J.A. Franek, B. Feng, B.L. Urquhart, R. Zhong, D.J. Freeman, B. Garcia, W.-P. Min, Reinstalling antitumor immunity by inhibiting tumor-derived immunosuppressive molecule IDO through RNA interference, J. Immunol. 177 (2006) 5639–5646.
[21] X. Liu, N. Shin, H.K. Koblish, G. Yang, Q. Wang, K. Wang, L. Leffet, M.J. Hansbury, B. Thomas, M. Rupar, P. Waeltz, K.J. Bowman, P. Polam, R.B. Sparks, E.W. Yue, Y. Li, R. Wynn, J.S. Fridman, T.C. Burn, A.P. Combs, R.C. Newton, P.A. Scherle, Selective inhibition of IDO1 effectively regulates mediators of antitumor immunity, Blood 115 (2010) 3520–3530.
[22] M.R. Mautino, F.A. Jaipuri, J. Waldo, S. Kumar, J. Adams, C. Van Allen, A. Marcinowicz-Flick, D.H. Munn, N. Vahanian, C.J. Link, NLG919, a novel indoleamine-2,3-dioxygenase (IDO)-pathway inhibitor drug candidate for cancer therapy. [abstract], Proceedings of the 104th Annual Meeting of the American Association for Cancer Research; 2013 Apr 6–10, Cancer Res, 73(8 Suppl), AACR, Washington, DC. Philadelphia (PA), 2013http://dx.doi.org/10.1158/1538-7445.AM2013-491 (Abstract nr 491, (2013)).
[23] O. Takikawa, T. Kuroiwa, F. Yamazaki, R. Kido, Mechanism of interferon-gamma action—characterization of indoleamine 2,3-dioxygenase in cultured human-cells induced by interferon-gamma and evaluation of the enzyme-mediated tryptophan degradation in its anticellular activity, J. Biol. Chem. 263 (1988) 2041–2048.
[24] A. Matin, I.M. Streete, I.M. Jamie, R.J.W. Truscott, J.F. Jamie, A fluorescence-based assay for indoleamine 2,3-dioxygenase, Anal. Biochem. 349 (2006) 96–102.
[25] P. Tomek, B. Palmer, J. Flanagan, S.-P. Fung, D.A. Bridewell, J. Jamie, L.-M. Ching, Formation of an N-formylkynurenine-derived fluorophore and its use for measuring indoleamine 2,3-dioxygenase 1 activity, Anal. Bioanal. Chem. 405 (2013) 2515–2524.
[26] A. Pirie, Formation of N′-formylkynurenine in proteins from lens and other sources by exposure to sunlight, Biochem. J. 125 (1971) 203–208.
[27] C.E. Dalgliesh, The synthesis of N′-formyl-DL-kynurenine, Nα-acetyl- DL-kynurenine and belated compounds, and observations on the synthesis of kynurenine, J. Chem. Soc. (1952) 137–141 (Resumed).
[28] R. Dick, B.P. Murray, M.J. Reid, M.A. Correia, Structure–function relationships of rat hepatic tryptophan 2,3-dioxygenase: identification of the putative heme-ligating histidine residues, Arch. Biochem. Biophys. 392 (2001) 71–78.
[29] L.W. Daasch, High resolution mass spectrum of piperidine, J. Phys. Chem. 69 (1965) 3196-3196.
[30] O. Calvez, A. Chiaroni, N. Langlois, Enantioselective synthesis of 2,3-disubstituted piperidines from (S)-methylpyroglutamate, Tetrahedron Lett. 39 (1998) 9447–9450.
[31] J. Lee, T. Hoang, S. Lewis, S.A. Weissman, D. Askin, R.P. Volante, P.J. Reider, Asymmetric synthesis of (2S,3S)-3-hydroxy-2-phenylpiperidine via ring expansion, Tetrahedron Lett. 42 (2001) 6223–6225.
[32] Y. Matsumura, D. Minato, O. Onomura, Highly enantioselective introduction of bis(alkoxycarbonyl)methyl group into the 2-position of piperidine skeleton, J. Organomet. Chem. 692 (2007) 654–663.
[33] G. Pelletier, L. Constantineau-Forget, A.B. Charette, Directed functionalization of 1,2-dihydropyridines: stereoselective synthesis of 2,6-disubstituted piperidines, Chem. Commun. 50 (2014) 6883–6885.
[34] L. Zhou, D.W. Tay, J. Chen, G.Y.C. Leung, Y.-Y. Yeung, Enantioselective synthesis of 2-substituted and 3-substituted piperidines through a bromoaminocyclization process, Chem. Commun. 49 (2013) 4412–4414.
[35] N.A. Stephenson, J. Zhu, S.H. Gellman, S.S. Stahl, Catalytic transamidation reactions compatible with tertiary amide metathesis under ambient conditions, J. Am. Chem. Soc. 131 (2009) 10003–10008.
[36] C.L. Allen, B.N. Atkinson, J.M.J. Williams, Transamidation of primary amides with amines using hydroxylamine hydrochloride as an inorganic catalyst, Angew. Chem. Int. Ed. 51 (2012) 1383–1386.
[37] T.B. Nguyen, J. Sorres, M.Q. Tran, L. Ermolenko, A. Al-Mourabit, Boric acid: a highly efficient catalyst for transamidation of carboxamides with amines, Org. Lett. 14 (2012) 3202–3205.
[38] S.P. Pathare, A.K.H. Jain, K.G. Akamanchi, Sulfated tungstate: a highly efficient catalyst for transamidation of carboxamides with amines, RSC Adv. 3 (2013) 7697–7703.
[39] L. Becerra-Figueroa, A. Ojeda-Porras, D. Gamba-Sánchez, Transamidation of carboxamides catalyzed by Fe(III) and water, J. Org. Chem. 79 (2014) 4544–4552.

Please cite this article as: P. Tomek, et al., Formation of fluorophores from the kynurenine pathway metabolite *N*-formylkynurenine and cyclic amines involves transamidation and carbon–carbon bond..., Biochim. Biophys. Acta (2015), http://dx.doi.org/10.1016/j.bbagen.2015.04.007